EUROPEAN FUSION DEVELOPMENT AGREEMENT
JET

EFDA–JET–PR(05)35

D. Testa, M. Cecconello, C. Schlatter, M. Adams, L. Bertalot, S. Conroy,
S. Popovichev, M. Santala and JET EFDA contributors

# The Dependence of the Proton-Triton Nuclear Reaction Rate on the Temperature and Energy Content of the High-Energy Proton Distribution Function

# The Dependence of the Proton-Triton Nuclear Reaction Rate on the Temperature and Energy Content of the High-Energy Proton Distribution Function

D.Testa[1], M.Cecconello[2], C.Schlatter[1], M.Adams[3], L.Bertalot[3,4], S.Conroy[5], S.Popovichev[3], M.Santala[6] and JET EFDA contributors*

*[1]CRPP, Association EURATOM – Confédération Suisse, EPFL, Lausanne, Suisse*
*[2]Division of Fusion Plasma Physics (Association EURATOM/VR), Alfvén Laboratory, Royal Institute of Technology, Stockholm, Sweden*
*[3]EURATOM/UKAEA Fusion Association, Culham Science Centre, Abingdon, OX14 3DB, UK*
*[3]Associazione Euratom-ENEA sulla Fusione, Frascati, I-00044, Roma, Italy*
*[5]INF, Uppsala University, EURATOM/VR Association, Uppsala, Sweden*
*[6]Helsinki University of Technology, Association Euratom – Tekes, Espoo, Finland*
** See annex of J. Pamela et al, "Overview of JET Results ", (Proc.20 th IAEA Fusion Energy Conference, Vilamoura, Portugal (2004).*

Preprint of Paper to be submitted for publication in
Plasma Physics and Controlled Fusion

## ABSTRACT

The endothermic nuclear reaction between thermal tritons and high energy protons can represent an important contribution to the total neutron yield in tokamak plasmas heated by radio-frequency waves, as previous JET experiments have demonstrated [7]. A detailed study is reported in a paper [2] in this issue. In this accompanying Letter we report the first systematic measurement of the scaling of the proton-Triton (pT) nuclear reaction rate as a function of the total energy content and perpendicular temperature of the fast protons heated by radio-frequency waves. It is found that the pT neutron rate increases almost linearly with the fast proton temperature and the total energy content, and appears to saturate when the fast proton energy is larger than ≈0.7MJ.

## INTRODUCTION

One of the nuclear reactions that can give rise to a significant source of neutrons in fusion plasmas is the endothermic $T(p,n)^3He$ one [1]: $T + p + 764keV \rightarrow n + {}^3He$. This proton-triton (pT) nuclear reaction requires a proton with energy in excess of $E_{pCM}$ = 764keV in the centre-of-mass reference frame. The detailed kinematics of the pT neutron production is described in the companion paper [2]. The high energy protons required to produce these pT neutrons are produced in the JET tokamak [3] via Ion Cyclotron Radio Frequency (ICRF) heating of the background minority hydrogen population. Due to the broad energy range of the fast protons produced by ICRF heating, the pT neutrons have also a broad energy spectrum, each neutron being produced at the energy $E_n = 0.75\times(E_{pCM}\text{-}764keV)$. For proton energies $E_{pCM}$>2MeV, this reaction has by far the highest cross-section between those typically occurring in fusion plasmas, i.e. those involving hydrogen isotope ions [1].

The interest in studying the pT nuclear reaction stems from the fact that a background hydrogen population is an unavoidable feature of tokamak plasmas with a first wall covered with carbon tiles, due to the structural properties of the CFC material [4]. In ITER, ICRF heating of the deuterium population is essentially considered as a tool to increase the ion temperature on the road to ignition [4]. However, the presence of a minority hydrogen population will also contribute to the total neutron rate through the pT nuclear reaction, and this needs to be properly considered when evaluating the various neutron production mechanisms as a tool to assess the plasma performance or infer background and fast ion plasma parameters such as the ion temperature and toroidal rotation [5]. Furthermore, the pT nuclear reaction has also been tentatively proposed as a possible tool for measuring the temperature of ICRF-driven protons in energy ranges where conventional methods, such as neutral particle analysis or γ-rays spectroscopy, are not available [2, 6]. Hence it is important to derive a scaling for the pT neutron rate $R_{pT}$ as function of the main features of the distribution function of the ICRF-driven high-energy protons $f_{pFAST}(E)$, such as their perpendicular temperature $T_{\perp pFAST}$ and total energy content $W_{pFAST}$.

A previous JET experiment has demonstrated the role of the pT nuclear reaction during ICRF heating of the minority proton distribution function in tritium-rich plasmas, $n_T/n_e$≈0.9 [7]. However, at that time it had not been possible to perform a systematic scan of the dependence of the pT neutron yield on $f_{pFAST}(E)$. A more systematic experimental study of the pT-neutrons in purely ICRF-heated plasmas with low tritium density (typically $n_T/n_e<0.01$) was performed in 2003 in JET during the Trace Tritium Experiments (TTE) [8, 9]. The main results of these pT experiments during the TTE campaign were initially reported in Ref.[6]; the general overview of these experiments is presented in the companion paper [2]. Here we concentrate on the scaling of the *excess pT-neutron rate* $R_{pT}$ as function of the core fast proton perpendicular temperature $T_{\perp pFAST,0}$ and total energy content $W_{pFAST}$ in such plasmas.

The excess pT-neutron rate $R_{pT}(t)$ is defined as $R_{pT}=R_{TOT}-(R_{DT}+R_{DD})-R_{ADD}$, where $R_{TOT}$ is the total (measured) neutron rate, $R_{DT}$ is the (measured) 14MeV neutron rate from the DT fusion reactions, $R_{DD}$ is the (measured) 2.5MeV neutron rate from the DD fusion reactions, and $R_{ADD}$ indicates possible (computed/measured) additional sources of neutrons in the energy range of the JET neutron detectors. Examples of possible contributions to $R_{ADD}$ have been described in Ref.[2], and these could introduce a large error in the inferred $R_{pT}$. However, as the background plasma parameters are almost constant over the various discharges that constitute our database, this error would only be of a systematic nature, hence by its very nature of no consequence for establishing the scaling laws which are the purpose of our experimental work. This is further demonstrated in a later section of this Letter.

Different detectors with often different time resolution were used to obtain the individually calibrated data $R_{TOT}$, $R_{DT}$ and $R_{DD}$ for the TTE experiments considered here. The total neutron rate $R_{TOT}$ was measured with three sets of fission chambers located around the Torus. Each set comprises a $U^{235}$ and a $U^{238}$ chamber operating in pulse-counting and current mode. The 2.5MeV neutron emission $R_{DD}$ was determined by the *neutron profile monitor* equipped with NE213 liquid scintillators and pulse shape discrimination hardware. Only neutron events within the energy range 1.8÷3.5MeV are detected, and a background subtraction is performed to eliminate events associated with higher energy neutrons (for instance, 14MeV DT-neutrons) that have slowed down, for instance due to scattering in the instrument itself. Two independent measurements of $R_{DT}$ were performed: with silicon diodes, using the threshold reactions Si(n,p) and Si(n, $\alpha$), applied routinely at JET as 14MeV neutron monitor; and with the newly installed Bicron scintillators, sensitive only to neutrons with $E_n>9$MeV, within the *neutron profile monitor* diagnostic system. A comprehensive and detailed overview of the various neutron diagnostics employed during the TTE experiments in JET is given in Refs.[10-15] and the references therein.

In order to combine the data coming from the different neutron detectors used for these experiments, hence deduce $R_{pT}(t)$, we have devised the procedure described below, which relies upon Gaussian propagation of the errors to track as accurately as possible the time evolution of the uncertainty on the computed $R_{pT}(t)$. First, we have integrated the calibrated data from each individual neutron detector over the longest time window between them all (typically 0.1 to 0.3s depending on the neutron counts) that was necessary to reduce the relative statistical error on each detector measurement (indicated by the subscript NX ) to less than $\sigma_{NX}$<10%. Such error $\sigma_{NX}$ was evaluated using the Poisson statistics on the neutron count: $\sigma=1/\sqrt{N}$, N being the total neutron count in the chosen time interval. Second, we have resampled these data over a 50ms-long time base (i.e., the typical time resolution of the $T_{\perp pFAST}$ measurements) using linear fitting routines for the steady-state phase of the discharge. This time base is now common to all neutron detectors. The error on each resulting time point was then determined by adding the 10% base error to the normalised ratio of the difference between the total neutron count on the short time interval ($C_{50ms}$) to the expectation value ($C_{EXP}$) which was obtained from averaging over the long time interval: $\sigma_{NX}=[0.01+(C_{50ms}-C_{EXP})^2/C_{EXP}^2]^{1/2}$. As a practical example to clarify this error propagation process, for an original 150ms-long time window used to obtain $\sigma_{NX}$<10%, with the total neutron count over the 150ms-long time window $C_{TOT}$, we have $C_{EXP}=C_{TOT}/3$. Third, we supplemented this steady-state analysis for transients such as the ICRF heating switch-on/off phases using guidance from available modelling for a set of similar discharges, such as that provided by the JETTO [16] and TRANSP [17] codes. This approach is useful to determine an empirical dependence of $R_{DD}(t)$ and $R_{DT}(t)$ during these transients as function of various plasma parameters such as the ion temperature, density, heating power and effective charge. This showed that the expected 2.5MeV DD neutron rate with ICRF-only heating and low ion temperature $T_i$<10keV scales linearly with the ICRF heating power $P_{RF}$, $R_{DD}\propto n_e^2 * P_{RF}/Z_{EFF}$, where $n_e$ is the electron density and $Z_{EFF}$ is the effective charge. On the other hand, the 14MeV DT neutron rate depends essentially on $n_T$ and on the presence of supra-thermal deuterons, as those obtained via Neutral Beam Injection (NBI): $R_{DT}(t)\propto n_e n_T * P_{NBI}/Z_{EFF}$, where $P_{NBI}$ is the NBI power. Therefore, to simplify our analysis, we have decided to ignore the NBI heating phase of all the discharges considered here, including a 300ms time window after the NBI switch-off to allow for the slowing-down of the high-energy NBI deuterons. Over this phase, we have therefore set $R_{pT}=0$ by default. We also note that $R_{pT}$ is typically very low at the start (end) of the ICRF heating phase, before (after) a steady-state $f_{pFAST}(E)$ is established (has decayed) over a few fast proton slowing-down times. Therefore even large statistical errors on the analysis of these transients do not actually affect the overall scaling derived here, for which the bulk of the data is obtained during steady-state phases.

It is also important to point out here that, due to the lack of accurate time-resolved measurement of the tritium concentration, we assumed a constant $n_T/n_e$, averaged over the steady-state ICRF heating phase of each individual discharge. Hence, $n_T$ was separately estimated by (a) time-integrating the tritium gas puff, (b) using the results of the JETTO and TRANSP simulations (when available), and (c) using the operational formula $n_T/n_D \approx R_{DT}/(R_{TOT}-R_{DT})/300$, which was used throughout the TTE experimental campaign to estimate the tritium concentration from the 14MeV neutron rate for an estimated ion temperature $T_i$=10keV. Note that $T_i$(keV)≈3÷5 for the experiments reported here, therefore the estimate (c) is in principle inaccurate, and it is mainly used here to provide a further constraint on the ratio $n_T/n_D$. The value of $n_T/n_e$ used in the analysis reported here comes from the averaging over the duration of the ICRF heating phase of these separate estimates, thus adding the further source of uncertainty $\sigma_{nT}$ to the calculation of $R_{pT}(t)$. The total relative statistical error on $R_{pT}(t)$ was therefore empirically determined as $\sigma_{RPT}=[\sigma_{RTOT}^2+\sigma_{RDD}^2+\sigma_{RDT}^2+\sigma_{nT}^2]^{1/2}$.

It is important to note here that the total neutron rate diagnostic ($R_{TOT}$) used for this analysis has a relatively low detection efficiency for neutrons of energy below ≈500keV [11], which constitute a large fraction of the pT-neutron spectrum. Hence, there is a significant (possibly up to a factor ≈2) systematic error on the resulting $R_{pT}(t)$, which clearly does not affect neither the statistical error on $R_{pT}(t)$ nor the scaling of $R_{pT}(t)$ vs. the fast proton temperature and total energy content reported here. This systematic error (and that coming from possible $R_{ADD}$) has on the other hand a detrimental impact on a possible diagnostic potential of the pT nuclear reaction [2, 6], for which an *exact and absolute* measurement of $R_{pT}(t)$ would obviously be needed.

The fast proton distribution function $f_{pFAST,0}(E)$, perpendicular temperature $T_{\perp pFAST,0}$ and density $n_{pFAST,0}$ were measured in the plasma core over the energy range $0.28\leq E(\text{MeV})\leq 1.1$ using a high-energy Neutral Particle Analyser (NPA) [18, 19]. A detailed description of the techniques used to infer $f_{pFAST,0}(E)$, $T_{\perp pFAST,0}$ and $n_{pFAST,0}$ from the measured atomic flux is given in Refs.[20-23]. Two different ICRF heating schemes were used in the experiments reported here: single-frequency (monochromatic) and multi-frequency (polychromatic). For monochromatic heating, the location of the peak ($R_{ABS}$) in the ICRF power deposition profile is on the magnetic axis ($R_{MAG}$). For the case of a strong first pass absorption, the RF power deposition profile can be very well approximated with a Gaussian shape with half-width at half-maximum ($w_{ABS}$) of the order of the Doppler shift of the resonance [22-25], hence giving $R_{ABS}=R_{MAG}$ and $w_{ABS}\approx$20cm. Using a similar argument for polychromatic heating, the total power deposition profile is given by the convolution of those obtained at each individual ICRF antenna frequency. The width of the power deposition profile can then be empirically approximated by the geometric mean of the sum of the Doppler width $w_{ABS}$ and the position of each $R_{ABS}$ weighted over the relative power density absorbed at the various location [25], giving the value $w_{ABS}\approx$35cm for the cases considered here. Hence, for the same proton density and ICRF power, the polychromatic heating scheme gives rise, in general, to a lower $T_{\perp pFAST}$ in the plasma core [25-27]. This can be understood by considering the Stix scaling $T_{\perp FAST}\propto\rho_{ABS}/n_{FAST}$ [24], where $\rho_{ABS}$ is the absorbed ICRF power density.

As typical examples of our measurements, we consider #61259 for the polychromatic heating case, and #61257 for the monochromatic heating case, respectively. Figure 1a shows the main plasma and ICRF heating parameters, and fig.1b shows the measured and fitted $\log_{10}(f_{pFAST,0}(E))$ at various time points of interest for #61259. Figure 2a and fig.2b show the same data for #61257. The NPA measurements were performed with a 4ms time resolution: the raw data were then integrated over 20-50ms, depending on the ion count rate, to obtain $f_{pFAST,0}(E)$ with a statistical error below <50%, hence a maximum error on the inferred $T_{\perp pFAST,0}$ not exceeding ≈15% [21]. By integrating $f_{pFAST,0}(E)$ over the energy range of the measurements, one then obtains $n_{pFAST,0}$. We have also verified the value of $n_{pFAST,0}$ using the magnetic measurement of the total fast ion energy content:

$$W_{pFAST} = \int dV n_{pFAST}(r)\left[T_{\perp pFAST}(r) + \frac{1}{2}T_{\| pFAST}\right] \approx 4.2\pi^2 a^2 R_{MAG}\int_1^1 dx x\kappa(x)\, n_{pFAST}(x)\, T_{\perp pFAST}(x) \quad (1)$$

Here x=r/a is the normalised minor radius, r being the radial coordinate along the plasma midplane, a is the plasma minor radius, and $T_{\| pFAST} \approx T_{\perp pFAST}/10$ [19, 22, 23]. Cylindrical geometry (without Shafranov shift) has been used to perform the volume integration: the JET toroidal geometry has been taken into account in a simplified form by considering only the elongation $\kappa(x)$ of the magnetic flux surfaces. It should be noted that this analytical result reproduces within the error bar of the magnetic measurements the full calculation of $W_{pFAST}$ considering the exact toroidal geometry [22, 23]. To evaluate Eq.1 we have used the $T_{\perp pFAST,0}$ and $n_{pFAST,0}$ as measured by the high energy NPA in the plasma core. We have assumed a Gaussian profile for $T_{\perp pFAST}(x)=T_{\perp pFAST,0}*\exp[-(x-x_{ABS})^2/w^2_{ABS}]$, with $x_{ABS}$ and $w_{ABS}$ given by ICRF power deposition [23, 25], and a parabolic profile for $n_{pFAST}(x)=n_{pFAST,0}*[0.05+0.95*(1-x^2)]$ [21, 22]. With this approach, and considering that the error on the magnetic measurement of $W_{pFAST}$ is of the order of 20%, we estimate the error on $n_{pFAST}$ to be of the order of 30%. For the polychromatic heating case #61259 we have that $T_{\perp pFAST,0} \approx 430$keV during the steady-state ICRF heating phase ($P_{RF}$=5.5MW, volume-average proton density $\langle n_{pFAST}\rangle \approx 1.4\times10^{17}m^{-3}$), compared to $T_{\perp pFAST,0} \approx 490$keV for #61257, the monochromatic heating case with higher $P_{RF}$=7.5MW and $\langle n_{pFAST}\rangle \approx 5\times10^{17}m^{-3}$. This is consistent with the expected lower $T_{\perp pFAST,0}$ for polychromatic heating for the same $P_{RF}$ and $\langle n_{pFAST}\rangle$.

Figures 3a and 3b show the measurements of the pT neutron rate for #61259 and #61257, respectively. In both these discharges approximately 3mg of tritium were puffed at the beginning of the ICRF heating phase, with some additional tritium from previous discharges due to recycling from the walls. We notice that the short 200ms blip of diagnostic NBI around t=48.5sec causes an approximately three-fold increase in $R_{TOT}$, due to the DT reactions.

Table 1 gives an overview of the ICRF heating and high energy proton parameters for all the seven discharges analysed in this work. In order to determine a scaling of $R_{pT}=f(T_{\perp pFAST}, W_{pFAST})$ we have focused our attention to time-windows with ICRF-only heating, i.e., removing the time window where the diagnostic NBI blip was applied, including 300ms at the end of the blip to allow for the slowing-down of the NBI ions. In particular, the data presented in Table 1 were averaged over the entire steady-state ICRF heating phase. Here $W_{pFAST}$ is the magnetic measurement of the fast proton energy content, $W_{FAST}=W_{DFAST}+W_{pFAST}$, $W_{FAST}=4(W_{DIA}-W_{PLASMA})/3$-*offset*, where $W_{DIA}$ is the diamagnetic energy and $W_{PLASMA}$ is the plasma stored energy and $W_{DFAST}$ is NBI fast ion energy (see the discussion in Ref.[28], Eq.10, which unfortunately has the wrong numerical coefficient due to a typo: note that by eliminating the NBI time window, no contribution to $W_{FAST}$ from the NBI high energy deuterons is expected, hence $W_{FAST}=W_{pFAST}$). Note also that we have set $R_{pT}$=0 over the NBI heating phase by default.

We notice from the comparison between fig.3a and fig.3b that the effect of the different heating scheme is mainly to change the fast proton temperature and energy content for a given $P_{RF}$ and $<n_{pFAST}>$. Hence, it is possible to combine the data from these two different experimental scenarios into one single database and compare the value of $R_{pT}$ simply as function of the fast ion temperature and energy content. Figure 4 presents the scaling of the measured $R_{pT}$ as function of $T_{\perp pFAST,0}$ and $W_{pFAST}$ for the data points obtained during the ICRF-only heating phase of the discharges indicated in Table 1. We note that the detailed kinematics of the pT-neutron production does not affect this scaling, as we are not considering the *precise details* of the neutron energy spectra (for instance: the number of pT-neutrons per unit solid angle in different energy ranges), but only the *total number* of measured pT-neutrons (i.e., the value integrated over the full energy range of the measurements made with the JET neutron detectors). We have focused our attention primarily to the data points collected over the steady-state heating phase, where typically $T_{\perp pFAST,0}$(keV)=250÷550. In addition to these points, which constitute the bulk of our data, we have also considered data points collected during the transient phases (ICRF power switch on/off) to provide boundary values for the $R_{pT}$ scaling at low $T_{\perp pFAST,0}$ and $W_{pFAST}$.

In fig.4 we have normalised $R_{pT}$ with respect to the tritium concentration $n_T/n_e$ and the fast proton concentration $<n_{pFAST}/n_e>$ (as given in Table 1) to take into account the changing (p, T) ion densities over the various discharges considered in this work. This removes from our database the obvious density dependency $R_{pT} \propto n_T n_{pFAST}$. We have then integrated the time-resolved $R_{pT}(t)$ over a sufficiently long time window (typically 50-100ms) to reduce the maximum statistical error on $R_{pT}(t)$ to no more than 30%. Finally, to remove some cluttering from fig.4, we have reduced the number of points by clustering the individual $R_{pT}=f(T_{\perp pFAST,0}, W_{pFAST})$ data points over a smaller number of close-by values of $T_{\perp pFAST,0}$ and $W_{pFAST}$, since values of $R_{pT} \pm \sigma_{RPT}$ are obtained for values of $T_{\perp pFAST,0}$ and $W_{pFAST}$ within their respective statistical error. Note that this approach conserves the database marginals, i.e. the global probability function in the reduced database for the measured $R_{pT}$ to be in a certain range of $T_{\perp pFAST,0}$ and $W_{pFAST}$ does not change by more than $\sigma_{RPT}/2$ in the original database. Therefore, the error bars shown in fig.4 are the sum of the uncertainties in the measurements together with the scatter in the original data, which was implicitly smoothed out through this clustering process.

Figure 4 shows that $R_{pT}$ increases almost linearly with $T_{\perp pFAST,0}$ for $T_{\perp pFAST,0}$>200keV, being very small and almost constant for $T_{\perp pFAST,0}$<200keV, consistent with the much lower number of protons with high energy $E_{pCM}$>764keV for lower $T_{\perp pFAST,0}$. The almost linear dependence $R_{pT} \propto T_{\perp pFAST,0}$ is not a trivial result: $R_{pT} \propto n_T n_{pFAST} \times <\sigma_{pT}(v) \upsilon_{pFAST}>$, averaged over the fast proton distribution function and integrated over the plasma volume. Similarly, $R_{pT}$ increases almost linearly with $W_{pFAST}$ up to $W_{pFAST} \approx$700kJ, and then shows some indication of possible saturation at higher $W_{pFAST}$, where many $R_{PT}$ points are bunched together for $W_{pFAST}$(kJ)=700→810. Since the range of the $W_{pFAST}$ measurements for the discharges considered here does not extend above $W_{pFAST} \approx$810kJ, it is however not possible to substantiate this experimental result more systematically.

Considering now the role of additional neutron producing mechanisms, summed up in the general $R_{ADD}$ term described earlier, we note that, when neglecting recycling from the walls, the first two discharges in our database should have $R_{pT}=0$ as there was no tritium gas puff. Hence, as a pessimistic estimate for such $R_{ADD}$, we can consider that all *supposed* pT neutrons for these two discharges must actually be accounted for by $R_{ADD}$, hence subtract this value from the other discharges as a background, and repeat the procedure described above to obtain fig.4. Figure 5 shows the result of this further analysis: we note that the approximately linear scaling of $R_{pT}=f(T_{\perp pFAST,0}, W_{pFAST})$ determined from fig.4 is maintained but now with a different offset. This confirms that even in the worst case, the various $R_{ADD}$ mechanisms are only introducing a systematic error in the analysis reported here.

## SUMMARY

In summary, the dependence of the pT neutron rate $R_{pT}$ has been analysed as a function of the core perpendicular fast proton temperature $T_{\perp pFAST,0}$ and proton energy content $W_{pFAST}$ for monochromatic and polychromatic ICRF heating. It is found that $R_{pT}$ increases almost linearly with $T_{\perp pFAST,0}$ in the range $200<T_{\perp pFAST,0}(\text{keV})<600$. No appreciable difference can be related to the different ICRF heating scheme, their main effect being that of producing a different $T_{\perp pFAST}(x)$. Similarly, $R_{pT}$ increases almost linearly with $W_{pFAST}$ only up to $W_{pFAST}\approx 700$kJ, and then appears to saturate at higher $W_{pFAST}$. This would be consistent with a depletion of fast protons from the plasma core at higher temperature.


## ACKNOWLEDGEMENTS

The authors would like to acknowledge the contribution of the whole JET experimental team, and in particular M.de Baar, P.Beaumont, J.Brzozowski, A.Murari, J.-M.Noterdaeme and V.Kiptily. This work has been conducted under the European Fusion Development Agreement. D.Testa was partly supported by the Fond National Suisse pour la Recherche Scientifique, Grant 620-062924.


## REFERENCES.


[1]. H.Liskien and A.Paulsen, Nucl. Data Tables **11** (1973), 569; see also http://www-nds.iaea.org/.

[2]. M.Santala et al., *Proton-triton fusion in ICRF-heated plasmas in JET*, this journal issue.

[3]. J.Wesson, *Tokamaks*, 3rd edition, (Oxford Science Publication, Oxford, 2003), p.617.

[4]. ITER Physics Basis Editors, Nucl. Fusion **39** (1999), 2137; 2004 issue, in preparation.

[5]. H.Henriksson et al., Plasma Phys. Control. Fusion **44** (2002), 1253; M.Tardocchi et al., Nucl. Fus. **42** (2002), 1273; H.Henriksson et al., Plasma Phys. Control. Fusion **47** (2005), 1763.

[6]. M.Santala et al., *pT fusion by RF-heated protons in JET trace tritium discharges*, Proceedings 31st EPS Conference on Controlled Fusion and Plasma Physics, London (UK), 2004.

[7]. M.Mantsinen et al., Nucl. Fusion **41** (2001), 1815.

[8]. K.-D.Zastrow et al., Plasma Phys. Control. Fusion **46** (2004), B255.

[9]. D.Stork et al., *Overview of transport, fast particle, heating and current-drive physics using tritium in JET plasmas*, OV-4/1, 20th IAEA Fusion Energy Conference, Vilamoura (Portugal), 2004; to appear in Nucl. Fusion, 2005.
[10]. L.Bertalot et al., *ITER relevant developments in neutron diagnostics during the JET Trace Tritium campaign*, Proceedings 23rd Symposium on Fusion Technology, Venice (Italy), 2004; to appear in Fusion Engineering and Design, 2005.
[11]. M.Swinhoe, O.Jarvis, Nucl. Instrum. Meth. **221** (1984), 460.
[12]. M.Loughlin et al., Rev. Sci. Instrum. **70** (1999), 1123.
[13]. B.Esposito et al., Rev. Sci. Instrum. **75** (2004), 3350.
[14]. S.Popovichev et al., *Performance of neutron measurements during JET trace tritium experiments*, Proceedings 31st EPS Conference on Controlled Fusion and Plasma Physics, London (UK), 2004.
[15]. Y.Kaschuck et al., *Neutron measurements during trace tritium experiments at JET using a stilbene detector*, Proceedings 31st EPS Conference on Controlled Fusion and Plasma Physics, London (UK), 2004.
[16]. G.Cenacchi, A.Taroni, *JETTO: a free-boundary plasma transport code*, Report ENEA-RT-T113-88-5, 1988.
[17]. R.Budny et al., Phys. of Plasmas **7** (2000), 5038.
[18]. A.Korotkov, A.Gondhalekar, 21st European Physical Society Conference on Controlled Fusion and Plasma Physics, Europhysics Conference Abstract 18-B(1994), I-266.
[19]. K.McClements et al., Nucl. Fusion **37** (1997), 473.
[20]. A.Korotkov et al., Nucl. Fusion **37** (1997), 35.
[21]. C.Schlatter et al., Rev. Sci. Instrum. **75** (2004), 3547.
[22]. D.Testa, A.Gondhalekar, Nucl. Fusion **40** (2000), 975.
[23]. D.Testa et al., Phys. Plasmas **6** (1999), 3498; and D.Testa et al., Phys. Plasmas **6** (1999), 3489.
[24]. T.Stix, *Waves in Plasmas*, (American Institute of Physics, New York, USA, 1992), chapter 17.
[25]. D.Testa et al., Plasma Phys. Control. Fusion **46** (2004), S59.
[26]. D.Testa et al., *Experimental studies of Alfven mode stability and wave-particle interaction in the JET tokamak*, Paper EX/P4-45, 20th IAEA Fusion Energy Conference, Vilamoura (Portugal), 2004.
[27]. M.Mantsinen et al., *Comparison of monochromatic and polychromatic heating in JET*, Proceedings 15th Topical Conference on Radio Frequency Power in Plasmas, Moran (USA), 2003.
[28]. L.-G. Eriksson et al., Nucl. Fus. **33** (1993), 1037.

| Shot | $R_{pT}$(neut/s) | $T_{puff}$ | $n_T/n_e$ | ICRF heating | $T_{\perp pFAST}$ | $<n_{pFAST}>$ | $W_{pFAST}$ |
|---|---|---|---|---|---|---|---|
| 61254 | $9.70\times10^{13}$ | *no puff* | 0.18% | 6.6÷7.2MW, mono | 450keV | $5.7\times10^{17}m^{-3}$ | 0.61MJ |
| 61256 | $1.21\times10^{14}$ | *no puff* | 0.15% | 6.3÷7.2MW, mono | 446keV | $5.9\times10^{17}m^{--3}$ | 0.73MJ |
| 61257 | $2.95\times10^{14}$ | 3.0mg | 0.35% | 7.1÷7.4MW, mono | 486keV | $4.8\times10^{17}m^{-3}$ | 0.68MJ |
| 61258 | $3.14\times10^{14}$ | 5.1mg | 0.42% | 7.4÷7.6MW, mono | 461keV | $5.4\times10^{17}m^{-3}$ | 0.69MJ |
| 61259 | $1.35\times10^{14}$ | 3.2mg | 0.50% | 4.6÷5.6MW, poly | 430keV | $1.4\times10^{17}m^{-3}$ | 0.59MJ |
| 61260 | $8.77\times10^{13}$ | 3.0mg | 0.63% | 4.3÷6.3MW, poly | 450keV | $2.2\times10^{17}m^{-3}$ | 0.55MJ |
| 61261 | $6.15\times10^{13}$ | 5.1mg | 0.89% | 2.7÷4.5MW, mono | 287keV | $6.5\times10^{17}m^{-3}$ | 0.31MJ |

*Table 1. Main plasma parameters for the set of discharges considered in this work.*

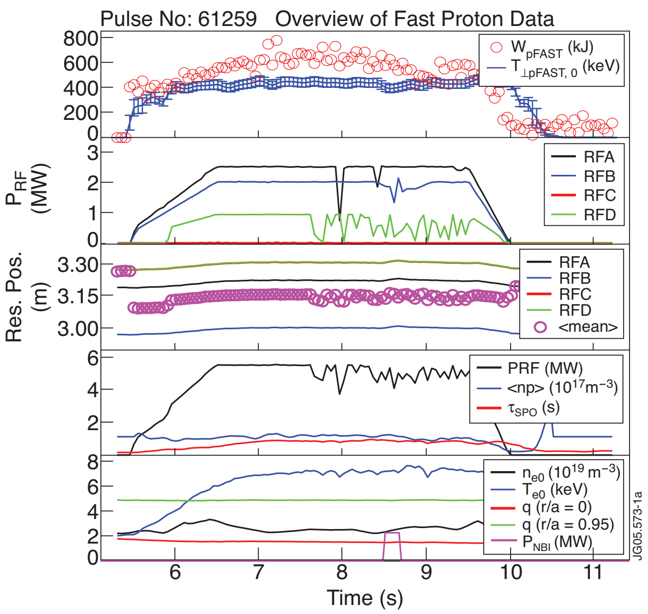


*Figure 1(a): Main plasma and ICRF heating parameters for Pulse No: 61259, the reference polychromatic heating case. Here RFx indicates the four ICRF generators, $\tau_{SP0}$ and $<n_p>$ are the core fast ion slowing down time and volume average proton density, respectively, $n_{e0}$ and $T_{e0}$ are the central electron density and temperature, q is the safety factor, and $W_{pFAST}$ is the magnetic measurement of the fast proton energy.*

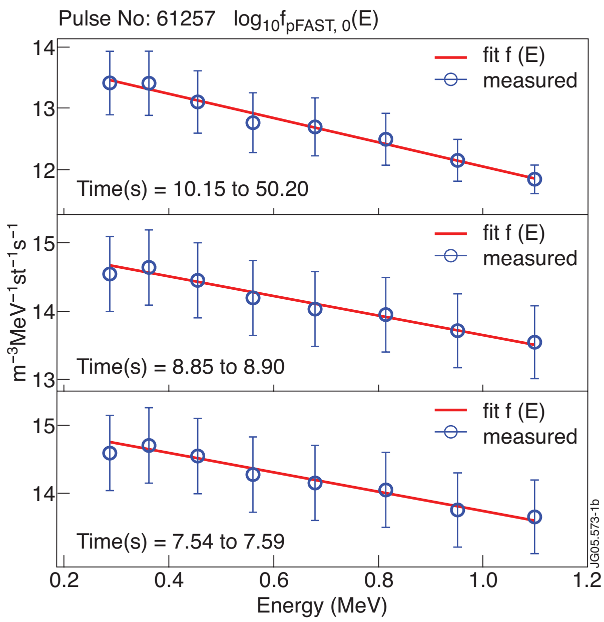


*Figure 1(b): The measured (markers) and fitted (line) fast ion distribution for Pulse No: 61259 at various time points of interest during the ICRF time window.*

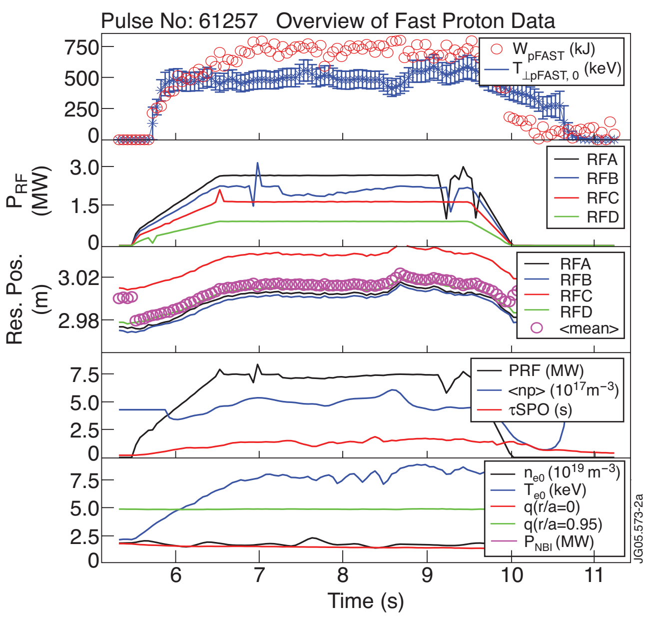


*Figure 2(a): Main plasma and ICRF heating parameters for Pulse No: 61257, the comparison monochromatic heating case at higher $P_{RF}$ and $<n_{pFAST}>$.*

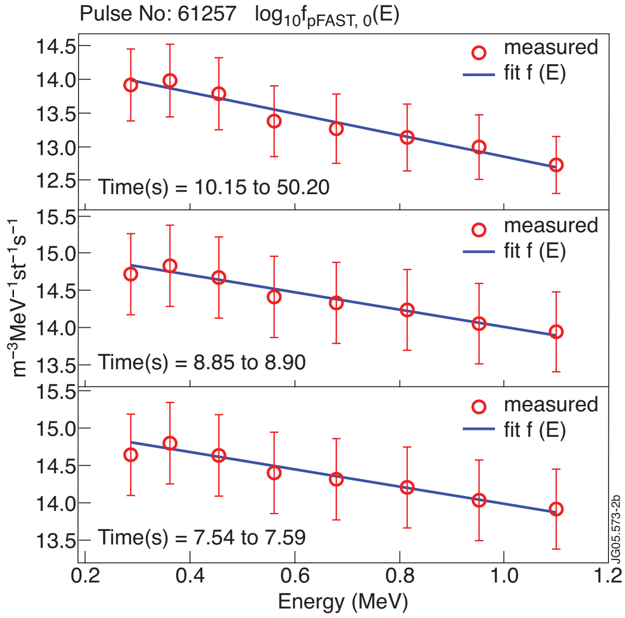


*Figure 2(b): The measured (markers) and fitted (line) fast ion distribution for Pulse No: 61257 at various time points of interest during the ICRF time window.*

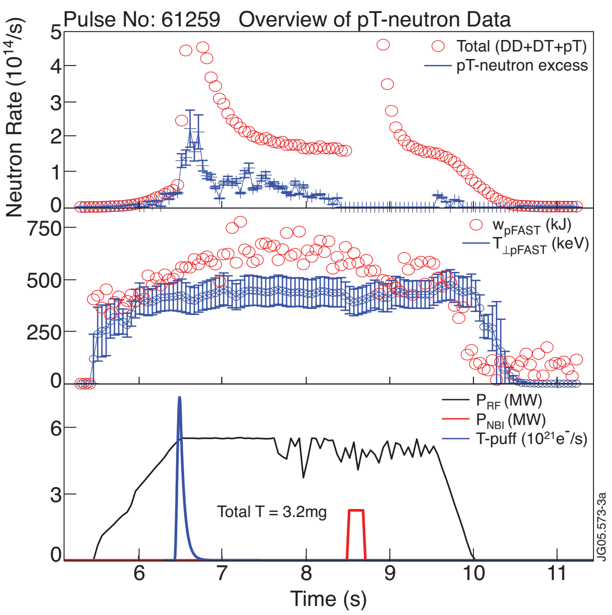


*Figure 3(a): The measured excess pT neutron rate for Pulse No: 61259. We notice the almost three-fold increase in the total neutron rate during the diagnostic NBI blip at t = 8.5sec (note that we set $R_{pT}$=0 by default over the NBI heating phase, including 300ms slowing-down time) and the almost two-fold increase in the $p_T$-neutrons after the tritium gas puff. As in fig.1a, $W_{pFAST}$ is the magnetic measurement of the fast proton energy content.*

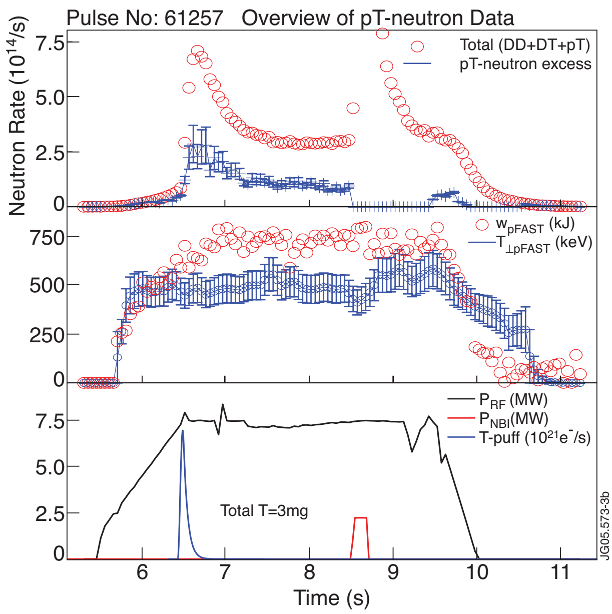


*Figure 3(b): The measured excess $p_T$ neutron rate for Pulse No: 61257, the monochromatic heating case. As in fig.2a, $W_{pFAST}$ is the magnetic measurement of the fast proton energy content. Note that $R_{pT}$=0 by default during the NBI heating phase, including 300ms ion slowing-down time after the NBI blip.*

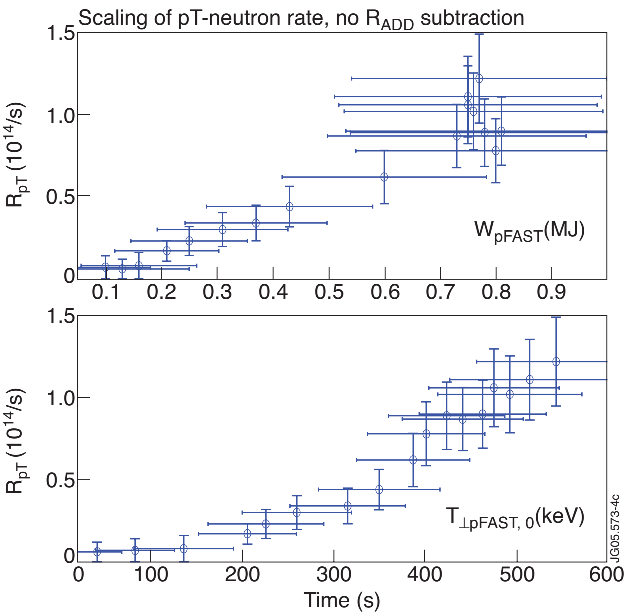


*Figure 4: Scaling of the measured $p_T$ neutron rate as a function of the fast proton temperature in the plasma core and the total fast proton energy content.*

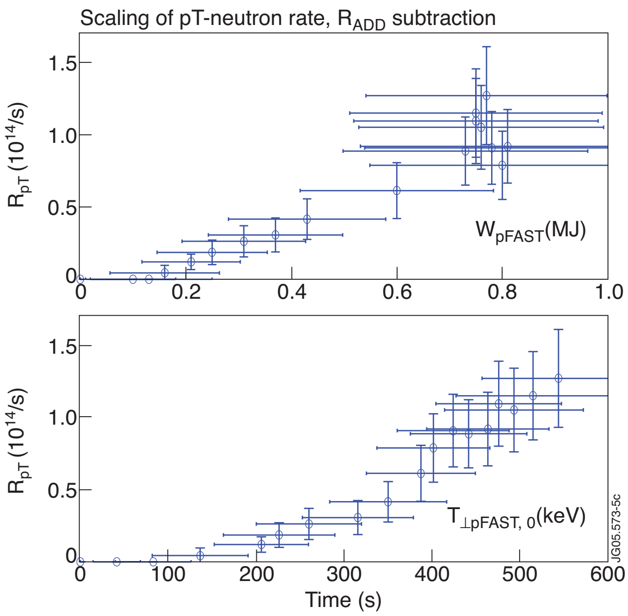


*Figure 5: Scaling of the measured $p_T$ neutron rate as a function of the fast proton temperature in the plasma core and the total fast proton energy content, subtracting the background $R_{ADD}$.*